Assessment of non-local effect on pressure term in RANS modeling using a DNS database

By R. Manceau[1], M. Wang AND P. Durbin

A DNS database for the channel flow at $Re_\tau = 590$ is used to investigate the validity of the hypotheses used to model the pressure term in the Reynolds stress transport equations by elliptic relaxation. It is shown that the correlation function involving the fluctuating velocity and the Laplacian of the pressure gradient, which is modeled by an exponential function, is actually not isotropic. It is not only elongated in the streamwise direction but also asymmetric in the direction normal to the wall. This feature is the main cause for the slight amplification of the redistribution between the Reynolds stress components in the log layer as predicted by the elliptic relaxation operator. The expected reduction in redistribution is predicted by a new formulation of the model, which can be derived by accounting for the asymmetry in the correlation function, without using any wall echo correction terms. The belief that this reduction is due to the wall echo effect is called into question through the present DNS analysis.

1. Introduction

During the past few decades, turbulence modelers mainly focussed on the pressure term in the Reynolds stress transport equations. In second moment closures, the production is exact and, accordingly, the pressure term is one of the most important terms to be modeled. Indeed, in a channel flow, this term is the main productive term in the equations for the diagonal Reynolds stresses except for the component in the streamwise direction, and balances the production term in the Reynolds shear stress equation (Mansour, Kim & Moin 1988).

Chou (1945) was the first to derive the integral equation of the pressure term from the Poisson equation for the pressure fluctuations and to distinguish between the slow part, rapid part and surface term (even though he did not use this terminology). For the rapid part, which involves the mean velocity gradient, he proposed to consider that the latter is locally a constant in order to be taken outside the integral. Since Chou's pioneering work, this approach has become very popular in the turbulence modeling community and the starting-point of all second moment closure models (e.g. Launder, Reece & Rodi 1975).

Bradshaw, Mansour & Piomelli (1987) assessed the validity of this local approximation for the rapid pressure using a DNS database. They showed that in the channel flow at $Re_\tau = 180$ (Kim, Moin & Moser 1987), this hypothesis is valid only

1 Laboratoire National d'Hydraulique, Electricité de France, 6 quai Watier 78 401 Chatou, France

for $y^+ \geq 40$. As a result, models based on it cannot be integrated down to the wall without modifications such as the introduction of damping functions.

In order to avoid the *ad hoc* damping functions, which are usually calibrated on experimental or DNS data with little theoretical basis, Durbin (1991) introduced a novel method. He proposed to model directly the two-point correlation in the integral equation of the pressure term, which preserves the non-local effect in the Reynolds stress transport equations. Then, he introduced the so-called elliptic relaxation approach, allowing the derivation of second moment closure models which can be integrated down to the wall without any damping functions.

While this method has led to very encouraging results, some room for improvement remains. One purpose of the present work is to assess the validity of the two-point correlation approximation, which was originally derived on an intuitive basis. Secondly, this work aims to assess the influence of the anisotropy of the two-point correlation on the pressure term in order to support future modifications of the model. Durbin's model assumes an isotropic shape for the correlation function, which may be the main improvable point of the method. These modeling issues will be examined using a channel flow DNS database at $Re_\tau = 590$ (Moser, Kim & Mansour 1998). In particular, the anisotropy of the correlation function will be explored, and the evolution of the length scale across the channel evaluated.

2. The pressure term in a channel

2.1. Integral equation of the pressure term

The pressure term which appears in the Reynolds stress equations is

$$\phi_{ij} = -\frac{1}{\rho}\left(\overline{u_j p_{,i}} + \overline{u_i p_{,j}}\right) \quad , \tag{1}$$

where ρ is the density, p is the fluctuating pressure, u_i are the fluctuating velocity components and $.{}_{,i}$ denotes derivative with respect to the x_i coordinate. The overline indicates ensemble average. Usually, ϕ_{ij} is split into two terms: the pressure-strain correlation and the pressure diffusion (Launder, Reece & Rodi 1975). However, the original form (1) of ϕ_{ij} will be used for the following reasons: first, Lumley (1975) showed that the decomposition is not unique and that this particular one is not the best one ; secondly, in the vicinity of a wall, the asymptotic behavior is not preserved for certain components. For instance, if $i = 1$ and 2 correspond respectively to the streamwise direction and the direction normal to the wall, the component ϕ_{12} behaves as y, whereas the pressure-strain and the pressure diffusion take a non-zero value at the wall. Therefore, in order to model correctly the total pressure term, it is necessary to model both terms of the decomposition such that their sum decreases as y in the vicinity of the wall.

The pressure fluctuation is the solution of the Poisson equation obtained by taking the divergence of the fluctuating part of the Navier-Stokes equations:

$$\nabla^2 p = -2\rho U_{i,j}\, u_{j,i} + \rho\left(\overline{u_i u_j} - u_i u_j\right)_{,ij} \quad , \tag{2}$$

where ∇^2 denotes the Laplacian operator and U_i the i^{th} component of the mean velocity. Since the differentiations are commutative, the gradient of the pressure fluctuation is also the solution of a Poisson equation:

$$\nabla^2 p_{,k} = -2\rho \left(U_{i,j}\, u_{j,i}\right)_{,k} + \rho \left(\overline{u_i u_j} - u_i u_j\right)_{,ijk} \quad . \tag{3}$$

In the following, the gradient of the pressure fluctuation will be assumed to satisfy the boundary condition $\partial p_{,k}/\partial \mathbf{n} = 0$, where $\mathbf{n}$ is the outgoing unit vector normal to the wall. This condition is not exact, but Kim (1989) uses this type of hypothesis for the pressure itself and showed that this is valid in the channel flow at $Re_\tau = 180$. In the present case, the same hypothesis can be applied to the pressure gradient, considering that its "Stokes part", i.e. the part produced by the inhomogeneous boundary condition, can be neglected.

The general solution of Eqs. (3) is

$$p_{,k}(\mathbf{x}) = -\int_\Omega \frac{\nabla^2 p_{,k}(\mathbf{x}')}{4\pi\|\mathbf{x}'-\mathbf{x}\|}\, dV(\mathbf{x}') - \int_{\partial\Omega} p_{,k}(\mathbf{x}') \frac{\partial}{\partial \mathbf{n}'}\left(\frac{1}{4\pi\|\mathbf{x}'-\mathbf{x}\|}\right) dS(\mathbf{x}') \ , \tag{4}$$

where bold letters $\mathbf{x}$ and $\mathbf{x}'$ denote position vectors, dV and dS the elementary volume and surface and $\partial\Omega$ the domain boundary.

Multiplying (4) by the fluctuating velocity and taking ensemble averaging, one can derive an integral equation for $\overline{u_j p_{,i}}$ and hence ϕ_{ij},

$$\rho\phi_{ij}(\mathbf{x}) = -\int_\Omega \left(\overline{u_j(\mathbf{x})\nabla^2 p_{,i}(\mathbf{x}')} + \overline{u_i(\mathbf{x})\nabla^2 p_{,j}(\mathbf{x}')}\right) \frac{dV(\mathbf{x}')}{4\pi\|\mathbf{x}'-\mathbf{x}\|} - \int_{\partial\Omega} \left(\overline{u_j(\mathbf{x}) p_{,i}(\mathbf{x}')} + \overline{u_i(\mathbf{x}) p_{,j}(\mathbf{x}')}\right) \frac{\partial}{\partial \mathbf{n}'}\left(\frac{1}{4\pi\|\mathbf{x}'-\mathbf{x}\|}\right) dS(\mathbf{x}') \ . \tag{5}$$

This equation will henceforth be referred to as the integral equation of the pressure term. It involves two-point correlations such as $\overline{u_j(\mathbf{x})\nabla^2 p_{,i}(\mathbf{x}')}$, which need to be modeled and are the main concern of this work.

In some situations, the surface integral in (4) can be transformed into a volume integral. For instance, in a semi-infinite space, bounded by an infinite plane, as considered by Launder, Reece & Rodi (1975), Eq. (4) can be written as

$$p_{,k}(\mathbf{x}) = -\int_\Omega \nabla^2 p_{,k}(\mathbf{x}') \left(\frac{1}{4\pi\|\mathbf{x}'-\mathbf{x}\|} + \frac{1}{4\pi\|\mathbf{x}'^*-\mathbf{x}\|}\right) dV(\mathbf{x}') \ , \tag{6}$$

where $\mathbf{x}'^*$ is the image term of $\mathbf{x}'$ by symmetry with respect to the plane. The function

$$G_\Omega(\mathbf{x},\mathbf{x}') = -\frac{1}{4\pi\|\mathbf{x}'-\mathbf{x}\|} - \frac{1}{4\pi\|\mathbf{x}'^*-\mathbf{x}\|} \tag{7}$$

is then called the Green function of the domain Ω.

In more general geometries, the Green function is unknown. In the particular case of a channel, the Green function is easy to derive only after taking Fourier transforms in x- and z-directions (Kim 1989). This spectral Green function is not useful for the present purpose: however, a form of (4) without surface integral will be needed in the following analysis, especially in §5.1, where the question of the wall echo effect will be investigated. The purpose of the next section is to derive a sufficiently good approximation of (4) which does not involve any surface integral.

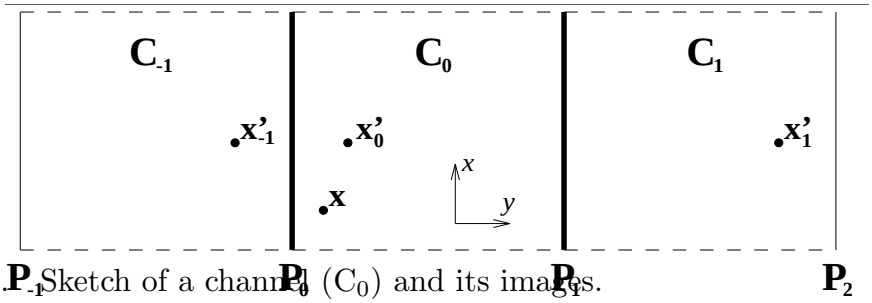

FIGURE 1. Sketch of a channel (C_0) and its images.

2.2. Approximation of the Green function in a channel

The simplest solution to eliminate the surface integral in (4) is to neglect it. Chou (1945) used this approximation but emphasized that all the conclusions which can be drawn are thus valid only at locations "not too close to the boundary of the moving fluid" because, in the vicinity of the wall, the weight of the surface integral has the same order of magnitude as the volume integral. This can be easily seen in the case of a semi-infinite domain bounded by a plane. In this case, Eq. (4) can be written as (6), which shows that if the fixed point $\mathbf{x}$ is sufficiently close to the wall, the principal term and the image term are almost equal. If $\mathbf{x}$ is exactly on the wall, the two terms are identical. Furthermore, Bradshaw (1973) noted that the order of magnitude of the image term is still 15% of the total when the correlation length scale is $L = \kappa y$, where κ is the Karman constant. The influence of this term will be assessed in §5.1. At this point, the surface integral cannot be neglected and therefore, in order to allow the following DNS analysis to be valid down to the wall, a less crude approximation than that used by Chou is needed.

Let us consider a channel C_0 bounded by two infinite planes P_0 and P_1 (Fig. 1). In this domain, the problem to solve is

$$\nabla^2 f = g \ , \tag{8}$$

with $f,_{\mathbf{n}} = 0$ on ∂C_0. Let us now consider the image channels C_{-1} and C_1 shown in Fig. 1, which are symmetrical to C_0 with respect to P_0 and P_1, respectively. Extending g by symmetry in C_{-1} and C_1, solving Eq. (8) in the domain $C_{-1} \cup C_0 \cup C_1$ and using all the symmetries, the solution can be shown to take the form

$$f(\mathbf{x}) = -\int_{C_0} H(\mathbf{x}, \mathbf{x'}_0)\ g(\mathbf{x'}_0)\ dV(\mathbf{x'}_0) \ - \int_{\partial C_0} \frac{\partial H(\mathbf{x}, \mathbf{x'}_0)}{\partial \mathbf{n'}}\ f(\mathbf{x'}_0)\ dS(\mathbf{x'}_0) \ , \tag{9}$$

with

$$H(\mathbf{x}, \mathbf{x'}_0) = \frac{1}{4\pi \|\mathbf{x'}_{-1} - \mathbf{x}\|} + \frac{1}{4\pi \|\mathbf{x'}_0 - \mathbf{x}\|} + \frac{1}{4\pi \|\mathbf{x'}_1 - \mathbf{x}\|} \ , \tag{10}$$

where $\mathbf{x'}_{-1}$ and $\mathbf{x}_1$ are the specular images of $\mathbf{x'}_0$ in P_0 and P_1 (Fig. 1), respectively. The surface integral in this expression can now be neglected. Indeed, on P_0, the derivative of $H(\mathbf{x}, \mathbf{x'}_0)$ can be evaluated:

$$\frac{\partial}{\partial \mathbf{n'}} H(\mathbf{x}, \mathbf{x'}_0) = \frac{\|\mathbf{x'}_{-1} - \mathbf{x}\| \cdot \mathbf{n'}}{4\pi \|\mathbf{x'}_{-1} - \mathbf{x}\|^3} - \frac{\|\mathbf{x'}_0 - \mathbf{x}\| \cdot \mathbf{n'}}{4\pi \|\mathbf{x'}_0 - \mathbf{x}\|^3} + \frac{\|\mathbf{x'}_1 - \mathbf{x}\| \cdot \mathbf{n'}}{4\pi \|\mathbf{x'}_1 - \mathbf{x}\|^3} \ . \tag{11}$$

Since $\mathbf{x'}_{-1} = \mathbf{x'}_0$, the sum of the two first terms is zero and hence the surface integral only involves the contribution of the image $\mathbf{x'}_1$, which is far from the point $\mathbf{x}$. Likewise, on the other wall P_1, the surface integral only contains the contribution of the image point on P_{-1}. This is in contrast to Chou's approximation, where the derivative in the neglected surface integral is equal to the second term of (11). It goes to infinity when $\mathbf{x'}_0 = \mathbf{x}$, giving to the surface integral the same weight as the volume integral. In the following analysis, the function $H(\mathbf{x}, \mathbf{x'}_0)$ will be used, considering it as a sufficiently good approximation of the Green function, even in the vicinity of the walls.

3. The elliptic relaxation method

By using the approximate Green function, the integral equation of the pressure term (5) can be written as

$$\rho\phi_{ij}(\mathbf{x}) = -\int_\Omega \left(\overline{u_j(\mathbf{x})\nabla^2 p_{,i}\,(\mathbf{x}')} + \overline{u_i(\mathbf{x})\nabla^2 p_{,j}\,(\mathbf{x}')}\right)\; H(\mathbf{x},\mathbf{x}')\; dV(\mathbf{x}')\;. \tag{12}$$

In this equation, two-point correlations between the fluctuating velocity and the Laplacian of the pressure gradient appear. Following Durbin (1991), in order to preserve the non-local effect, they can be modeled as

$$\overline{u_n(\mathbf{x})\nabla^2 p_{,m}\,(\mathbf{x}')} = \overline{u_n(\mathbf{x}')\nabla^2 p_{,m}\,(\mathbf{x}')}\exp\left(-\frac{\|\mathbf{x}'-\mathbf{x}\|}{L}\right)\;, \tag{13}$$

where L is the correlation length scale. The validity of this hypothesis will be scrutinized in §5.2 using a DNS database. Here, the rationalization of the elliptic relaxation equation is analyzed in the context of channel flow.

Durbin (1991) used Chou's approximation, which excludes the image terms in $H(\mathbf{x},\mathbf{x}')$. The integral equation of the pressure term, combined with the model (13), becomes

$$\rho\phi_{ij}(\mathbf{x}) = -\int_\Omega (\overline{u_j(\mathbf{x}')\nabla^2 p_{,i}\,(\mathbf{x}')} + \overline{u_i(\mathbf{x}')\nabla^2 p_{,j}\,(\mathbf{x}')})\underbrace{\frac{\exp\left[-\dfrac{\|\mathbf{x}'-\mathbf{x}\|}{L}\right]}{4\pi\|\mathbf{x}'-\mathbf{x}\|}}_{E(\mathbf{x},\mathbf{x}')} dV(\mathbf{x}')\;. \tag{14}$$

The function $E(\mathbf{x},\mathbf{x}')$ is the free-space Green function associated with the operator $-\nabla^2 + 1/L^2$. Hence, (14) is the solution of the following Yukawa equation*:

$$\phi_{ij} - L^2\nabla^2\phi_{ij} = -\frac{L^2}{\rho}(\overline{u_j\nabla^2 p_{,i}} + \overline{u_i\nabla^2 p_{,j}})\;. \tag{15}$$

* In 1935, Yukawa was the first to apply this inversion in physics to solve the equation of interaction potential between particles.

Noting that in quasi-homogeneous situations, the second term on the LHS of this equation vanishes, Durbin proposed to use a quasi-homogeneous model ϕ_{ij}^h instead of the RHS. This leads to the following elliptic relaxation model for ϕ_{ij}:

$$\phi_{ij} - L^2 \nabla^2 \phi_{ij} = \phi_{ij}^h \ . \tag{16}$$

Any quasi-homogeneous model, such as LRR model or SSG model, can be used for ϕ_{ij}^h, thus allowing the extension of these models down to solid boundaries. Indeed, (16) is valid down to the wall, when appropriate boundary conditions for ϕ_{ij} are provided (Durbin 1993).

However, Eq. (14) does not give rigorously the solution of (15) in a plane channel. Analogous to the Green function for the Laplacian operator, the Green function associated with the Yukawa operator must at least be approximated using the image points with respect to the walls. Thus, a better approximation to the solution of (15) is

$$\rho\phi_{ij}(\mathbf{x}) = -\int_\Omega (\overline{u_j(\mathbf{x'}_0)\nabla^2 p_{,i}(\mathbf{x'}_0)} + \overline{u_i(\mathbf{x'}_0)\nabla^2 p_{,j}(\mathbf{x'}_0)})$$
$$\left(\frac{\exp\left[-\dfrac{\|\mathbf{x'}_{-1}-\mathbf{x}\|}{L}\right]}{4\pi\|\mathbf{x'}_{-1}-\mathbf{x}\|} + \frac{\exp\left[-\dfrac{\|\mathbf{x'}_0-\mathbf{x}\|}{L}\right]}{4\pi\|\mathbf{x'}_0-\mathbf{x}\|} + \frac{\exp\left[-\dfrac{\|\mathbf{x'}_1-\mathbf{x}\|}{L}\right]}{4\pi\|\mathbf{x'}_1-\mathbf{x}\|} \right) dV(\mathbf{x'}_0) \ . \tag{17}$$

Now, using the approximation (13) for the two-point correlations, the integral equation of the pressure term (12) does not lead to (17) but to the following equation:

$$\rho\phi_{ij}(\mathbf{x}) = -\int_\Omega (\overline{u_j(\mathbf{x'}_0)\nabla^2 p_{,i}(\mathbf{x'}_0)} + \overline{u_i(\mathbf{x'}_0)\nabla^2 p_{,j}(\mathbf{x'}_0)})$$
$$\left(\frac{\exp\left[-\dfrac{\|\mathbf{x'}_0-\mathbf{x}\|}{L}\right]}{4\pi\|\mathbf{x'}_{-1}-\mathbf{x}\|} + \frac{\exp\left[-\dfrac{\|\mathbf{x'}_0-\mathbf{x}\|}{L}\right]}{4\pi\|\mathbf{x'}_0-\mathbf{x}\|} + \frac{\exp\left[-\dfrac{\|\mathbf{x'}_0-\mathbf{x}\|}{L}\right]}{4\pi\|\mathbf{x'}_1-\mathbf{x}\|} \right) dV(\mathbf{x'}_0) \ . \tag{18}$$

Hence, the modeled pressure term (18) does not rigorously satisfy the Yukawa Eq. (15). However, the main contribution of the image terms to the integral corresponds to point $\mathbf{x'}_0$ near the walls. For instance, the weight of the first image term is important when $1/4\pi\|\mathbf{x'}_{-1}-\mathbf{x}\|$ has the same order of magnitude as $1/4\pi\|\mathbf{x'}_0-\mathbf{x}\|$, i.e., very close to the wall, where $\mathbf{x'}_{-1} \simeq \mathbf{x'}_0$. Then, the exponential factors $\exp(-\|\mathbf{x'}_{-1}-\mathbf{x}\|/L)$ and $\exp(-\|\mathbf{x'}_0-\mathbf{x}\|/L)$ are almost equal as well. Therefore, even considering that the Green function in a channel must be at least approximated by $H(\mathbf{x},\mathbf{x'})$, rather than using Chou's approximation, the elliptic relaxation model for the pressure term (16) can be considered as valid, as long as the model for the two-point correlations (13) is valid itself.

4. Focus and description of the DNS assessment

4.1 Issues to examine in the elliptic relaxation method

The elliptic relaxation approach is based on a unique hypothesis, namely the approximation (13) of the two-point correlations. This approximation was originally introduced intuitively by Durbin (1991) in order to preserve the dependence of the pressure term on all the points of the domain, leading to the well known non-local effect in the Reynolds stress equations.

The standard way (Monin & Yaglom 1975) of defining a correlation function f to be used in (12) is by writing the two-point correlations as

$$\overline{u_j(\mathbf{x})\nabla^2 p_{,i}\left(\mathbf{x}'\right)} + \overline{u_i(\mathbf{x})\nabla^2 p_{,j}\left(\mathbf{x}'\right)} = (\overline{u_j(\mathbf{x})\nabla^2 p_{,i}\left(\mathbf{x}\right)} + \overline{u_i(\mathbf{x})\nabla^2 p_{,j}\left(\mathbf{x}\right)})\ f(\mathbf{x},\mathbf{x}')\ . \tag{19}$$

In this expression, the one-point correlation is expressed in $\mathbf{x}$, i.e., the point where the velocities are evaluated in the two-point correlation. Then, it can be moved outside the integral in (12), which leads to the loss of the non-locality of the pressure term. However, this formulation allows the definition of the following length scale:

$$L(\mathbf{x})^2 = \int_\Omega f(\mathbf{x},\mathbf{x}')H(\mathbf{x},\mathbf{x}')dV(\mathbf{x}')\ , \tag{20}$$

which is an integral scale, since it provides the ratio between the integral and the correlation at zero separation:

$$\rho\phi_{ij} = -L^2(\overline{u_j(\mathbf{x})\nabla^2 p_{,i}\left(\mathbf{x}\right)} + \overline{u_i(\mathbf{x})\nabla^2 p_{,j}\left(\mathbf{x}\right)})\ . \tag{21}$$

In order to preserve the non-local effect, the correlation function must be defined in the following way:

$$\overline{u_j(\mathbf{x})\nabla^2 p_{,i}\left(\mathbf{x}'\right)} + \overline{u_i(\mathbf{x})\nabla^2 p_{,j}\left(\mathbf{x}'\right)} = (\overline{u_j(\mathbf{x}')\nabla^2 p_{,i}\left(\mathbf{x}'\right)} + \overline{u_i(\mathbf{x}')\nabla^2 p_{,j}\left(\mathbf{x}'\right)})\ f(\mathbf{x},\mathbf{x}')\ . \tag{22}$$

The only difference between (19) and (22) is the point where the one-point correlation is evaluated. If (22) is used in (12), the single-point correlation cannot be taken outside the integral. But the decomposition of the two-point correlation into the one-point correlation evaluated at $\mathbf{x}'$ and the correlation function, and the modeling of the latter as a function which solely depends on the difference $\mathbf{x}'-\mathbf{x}$, allows the conversion of the integral to a convolution product. Thus, Eq. (12) can be inverted, leading to (15). The feature which is used here is that $-\nabla^2\delta+\delta/L^2$, where δ is the Dirac function, is equal to the inverse of $\exp(-r/L)/r$ for the convolution product. Hence, the non-local effect is preserved through the Yukawa operator.

The shape of the correlation function defined by (22) has never been assessed before. The first purpose of this work is then to check if the approximation $f(\mathbf{x},\mathbf{x}') = \exp(-\|\mathbf{x}'-\mathbf{x}\|/L)$ is consistent with the DNS data. For instance, the correlation function in (22) is not prevented from being larger than 1. If the root-mean square of the velocity fluctuation u_n varies rapidly in one direction, $\overline{u_n(\mathbf{x})\nabla^2 p_{,m}\left(\mathbf{x}'\right)}$

can become larger than $\overline{u_n(\mathbf{x}')\nabla^2 p_{,m}(\mathbf{x}')}$. On the other hand, the correlation between the velocity and the Laplacian of the pressure gradient should decrease very rapidly with increasing separations and hence, the correlation function should remain smaller or only slightly larger than one.

The length scale used in the approximation (13) is not rigorously an integral scale because it does not satisfy (21). Nevertheless, it is the integral of the function $\exp(-r/L)$ from zero to infinity. One may attempt to evaluate this length scale as the integral of the correlation function $f(\mathbf{x}, \mathbf{x}')$. However, as will be shown in §5.4, this definition is not satisfactory. Thus, another purpose of the present work is to evaluate alternative definitions of the length scale, and compare it with the turbulent length scale $k^{3/2}/\varepsilon$, which is used in elliptic relaxation models.

The ultimate objective of the evaluations of the correlation function and the length scale is to find ways to improve the elliptic relaxation approach. As pointed out by Wizman *et al.* (1996), the elliptic relaxation equation does not act in the right direction in the log layer. For instance, if the IP and Rotta models are used as the source term in (16), since the anisotropy is fairly constant in the log layer, ϕ_{ij} has the same behavior in $1/y$ as ε and P. Then, it can be easily shown that the solution of (16) is

$$\phi_{ij} = \frac{1}{1 - 2C^2\kappa^2}\phi_{ij}^h \ , \tag{23}$$

if the length scale is $L = C\kappa y$, where κ is the Karman constant. Hence, in the log layer, the redistribution of energy between the components of the Reynolds stress tensor is amplified, while a damping due to the presence of the wall is expected.

Therefore, Wizman *et al.* (1996) introduced other formulations of the elliptic relaxation equation. The first one, the so-called *neutral formulation*, is defined as

$$\phi_{ij} - \nabla^2(L^2\phi_{ij}) = \phi_{ij}^h \ . \tag{24}$$

It produces neither amplification nor reduction of the redistribution in the log layer, since it leads to $\phi_{ij} = \phi_{ij}^h$. The second one, which yields the best agreement with DNS data, is given by

$$\phi_{ij} - L^2\nabla\left(\frac{1}{L^2}\nabla(L^2\phi_{ij})\right) = \phi_{ij}^h \ . \tag{25}$$

It exhibits a damping of the redistribution in the log layer.

These empirically derived new formulations require further justifications. What is suspected here is that the approximation of the correlation function f by an exponential function is not appropriate. Indeed, the latter is isotropic, whereas the former may decrease more rapidly when the point $\mathbf{x}'$ is moving towards the wall than when it is moving away from it. Experiments from Sabot (1976) in a pipe show that the contours of the two-point correlations of velocities are tightly packed between the point of zero separation and the wall. It is suspected that the same phenomenon occurs for correlations between velocity and Laplacian of the pressure gradient. Moreover, this feature is closely linked to the variation of the

length scale in the near wall region. When the correlation function is modeled by an isotropic function, the same weight is given to points towards the wall and those away from it. Since the source term decreases in the log layer, it results in an over-prediction of the integral. This phenomenon can be suspected to be the reason for the erroneous behavior of the elliptic relaxation equation in the log layer. This idea will be carefully explored in the following DNS analysis, in order to support modifications of the model such as those proposed by Wizman *et al.* (1996).

In addition, some general improvements of the model can be expected from such reformulations. Because of the erroneous behavior described above, it is difficult to reproduce accurately both the viscous sublayer and log layer. For instance, the coefficients of the V2F model have been tuned as a compromise between the boundary layer and the channel flow, since it is impossible to predict perfectly both flows with the same set of coefficients. Furthermore, this type of compromise limits the influence of the elliptic relaxation equation to a region very close to the wall. Parneix, Laurence & Durbin (1998) showed that in the case of the backstep flow, the turbulent force $-\overline{uv}_{,y}$ in the mean streamwise velocity equation is over-predicted in the backflow region, which acts to slow down the flow, leading to an under-prediction of the intensity of the recirculation. All modifications of the coefficients attempted by them proved ineffective, and they only managed to reduce the error by 50% by including terms involving the gradient of the mean flow in the turbulent transport term. In this case some improvement can be expected too by extending the influence of the elliptic relaxation equation in the backflow region and particularly by reformulating this equation in order to account for the variations of the length scale.

4.2 Channel flow database and post-processing

Since the Laplacian of the pressure gradient, which involves three spatial derivatives, will be calculated, a very accurate DNS database is needed. The database used in this study is the most recent channel flow simulation of Moser, Kim & Mansour (1998) at $Re_\tau = 590$. This flow was computed on a grid of $384 \times 257 \times 384$ points in streamwise (x), wall normal (y) and spanwise (z) directions, respectively. The computational domain is given by $2\pi\delta$, 2δ and $\pi\delta$ in x, y and z, where δ denotes the channel half-width. The simulation code employed a spectral method (Fourier series in x and z, and Chebychev polynomial in y) for spatial derivatives, and a semi-implicit scheme for time integration. A total of 75 fields (restart files) are available for statistical averaging.

In order to assess the shape of the correlation function f defined by (22), the two-point correlations between the fluctuating velocities and the Laplacian of the pressure gradient must be calculated. They are evaluated in the following manner:

- First, the Laplacian of the total pressure gradient is evaluated directly from the velocity field, $\nabla^2\widetilde{p} = -\widetilde{u}_{i,j}\,\widetilde{u}_{j,i}$ where $\widetilde{.}$ denotes total quantities. The spatial derivatives are calculated using the same Fourier/Chebychev spectral method as for the DNS.
- The one-point and two-point correlations between the gradient of the Laplacian of the total pressure and the velocity components $\overline{\widetilde{u}_j(\mathbf{x}')\nabla^2\widetilde{p}_{,i}\,(\mathbf{x}')}$ and $\overline{\widetilde{u}_j(\mathbf{x})\nabla^2\widetilde{p}_{,i}\,(\mathbf{x}')}$

are then computed. The gradient is calculated using Fourier spectral derivatives in x and z, and fourth order finite differences in y.

- The corresponding mean quantities involving U_i and $\nabla^2 P_{,i}$ are calculated. They are finally subtracted out from correlations between total quantities in order to obtain the correlations between fluctuating quantities.

The ensemble averages are replaced by averaging in the homogeneous directions and over the 75 restart fields. The computations are very expensive. As a practical matter, calculations are performed at 7 representative y-locations only, for separations in x-y, x-z, y-z planes.

5. Results and discussion

5.1 The wall echo

Since the paper of Launder, Reece & Rodi (1975), it has been widely accepted in the turbulence community that, in a semi-infinite space bounded by a plane at $y = 0$, the image term in the integral equation of ϕ_{ij} represents the so-called wall echo effect, responsible for the reduction of the amplitude of the energy redistribution between components of the Reynolds stress tensor. Consequently, in second moment closure models, extra terms are frequently incorporated to account for this effect (Gibson & Launder 1978). These wall echo terms depend on the distance to the wall, which is often not well defined in complex geometries. The inclusion of wall echo terms often worsen the predictions in engineering applications even though they have proven to be effective in simple flows.

The physical reasoning behind this is that the pressure fluctuations are reflected by the wall, introducing an "echo" contribution which can be considered as instantaneous in an incompressible flow. Considering each point of the domain as a source of pressure fluctuations, the echo can be represented by an image source of fluctuations. The contribution of this echo actually increases the pressure fluctuations (in a closed room, the echo increases the noise). This feature is linked to the homogeneous Neumann boundary condition at the wall. Mathematically, this can be related to the fact that the presence of the wall induces the presence of an image term in the Green function (7). On account of the homogeneous Neumann boundary condition, the image term appears with the same sign as the principal term, whereas if a homogeneous Dirichlet boundary condition was satisfied at the wall, it should have an opposite sign.

Thus, the wall echo effect cannot be responsible for the damping of the energy redistribution. Figure 2 shows a comparison among the three source terms in the integral Eq. (12) of the pressure term, corresponding to the three parts in $H(\mathbf{x}, \mathbf{x'}_0)$ (cf. (10)), for the components ϕ_{11} and ϕ_{22}. The magnitudes of these source terms have been arbitrarily normalized such that the maximum of the first image term ($n = -1$) is 1. The solid line, representing the principal term ($n = 0$), has been truncated because it approaches infinity at $y^+ = y'^+ = 30$. It is clear that the first image term ($n = -1$), associated with the closer wall located at $y^+ = 0$, is always of the same sign as the principal term. It can also be noticed that this term gives more weight to the region very close to the wall, where it becomes equal to the

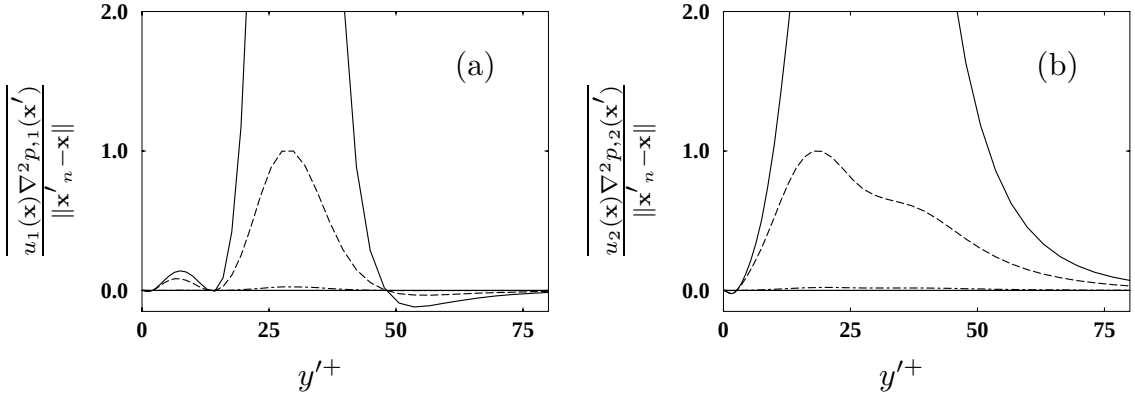

FIGURE 2. Comparisons of the different source terms in the integral Eq. (12) of the pressure term with $H(\mathbf{x}, \mathbf{x'}_0)$ given by (10) at location $y^+ = 30$. Separations in x- and z-directions are zero. (a) ϕ_{11}; (b) ϕ_{22}. ——— n=0 (principal term); – – – – n=-1 (first image term); —·— n=1 (second image term). The vertical coordinate is arbitrarily normalized such that the maximum of $n = -1$ term is 1.

principal term and the two-point correlation changes sign for the component ϕ_{22}, as shown in Fig. 2b. However, this feature is not present in Fig. 2a and, moreover, the contribution of this part of the domain to the integral is rather small. It must be emphasized that even though the $n = -1$ source term appears negligible near the point of zero separation relative to the $n = 0$ term, which goes to infinity, its contribution to the integral is significant. Indeed, the value of the volume integral of $1/r$ between $r = 0$ and $r = 1$ is only 2π. Thus, Figs. 2a and 2b clearly show that the contributions of the image terms to the integral are of the same sign as the contribution of the principal term. Unfortunately, it is not possible here to evaluate quantitatively the relative weight of each term because it involves two-point correlations with separations in the whole 3D-domain, which have not been calculated.

At this point a very interesting conclusion can be drawn. The image terms in the integral Eq. (12) with $H(\mathbf{x}, \mathbf{x'})$ defined by (10), which account for the wall echo, actually have an amplification effect on the redistribution of turbulent energy between the different component of the Reynolds stress. Thus, it is time to abandon the traditional way of modeling the damping of the redistribution, which consists of introducing Gibson & Launder (1978) type terms involving functions of the geometry. This damping can only be caused by the damping of the two-point correlation itself, which is a consequence of the no-slip boundary conditions and the wall-blocking effect.

This phenomenon is an inhomogeneity effect, which can only be accounted for by non-local models, such as the elliptic relaxation model. However, it has been shown in §4.1 that the behavior of the latter is not satisfactory in the log layer. The following sections will show that this flaw is due to the fact that the model does not account for the asymmetry of the correlation function in the direction normal to the wall, which is a consequence of the variation of the length scale in inhomogeneous regions. By reformulating the elliptic relaxation equation, the damping of

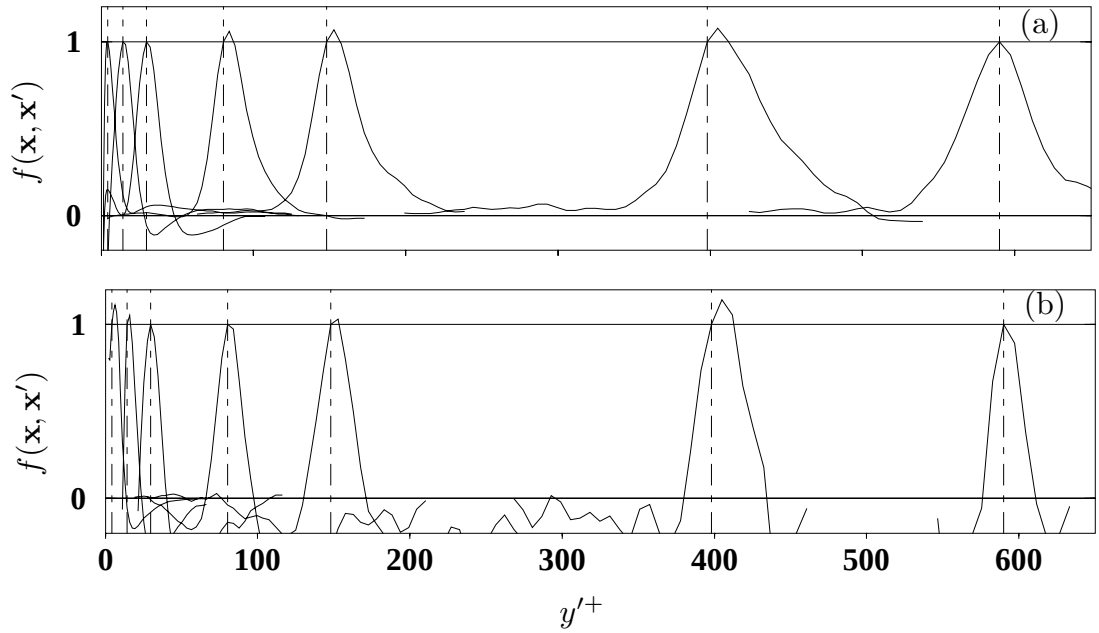

FIGURE 3. Correlation function defined by (26) calculated from the DNS data at different y locations: $y^+ = 4$; $y^+ = 14$; $y^+ = 30$; $y^+ = 80$; $y^+ = 150$; $y^+ = 400$; $y^+ = 590$. Separations in x- and z-directions are zero. (a) $f(\mathbf{x},\mathbf{x}') = \overline{u_1(\mathbf{x})\nabla^2 p_{,1}(\mathbf{x}')}/\overline{u_1(\mathbf{x}')\nabla^2 p_{,1}(\mathbf{x}')}$; (b) $f(\mathbf{x},\mathbf{x}') = \overline{u_2(\mathbf{x})\nabla^2 p_{,2}(\mathbf{x}')}/\overline{u_2(\mathbf{x}')\nabla^2 p_{,2}(\mathbf{x}')}$.

the redistribution in the log layer can be reproduced, without introducing any "wall echo" correction term (§6.2).

5.2 Asymmetry of the correlation function in y-direction

The main purpose of this study is to investigate through DNS data the shape of the correlation function defined by (22), which is modeled by an exponential function in the elliptic relaxation method. First, it must be emphasized that this model function is unique, i.e., it does not depend on the component of ϕ_{ij}. This feature is not supported by any theoretical result, but is necessary to warrant the frame independence of the model. On the other hand, using DNS data, a correlation function $f(\mathbf{x},\mathbf{x}')$ can be calculated for each component of ϕ_{ij}:

$$f(\mathbf{x},\mathbf{x}') = \frac{\overline{u_\alpha(\mathbf{x})\nabla^2 p_{,\beta}(\mathbf{x}')} + \overline{u_\beta(\mathbf{x})\nabla^2 p_{,\alpha}(\mathbf{x}')}}{\overline{u_\alpha(\mathbf{x}')\nabla^2 p_{,\beta}(\mathbf{x}')} + \overline{u_\beta(\mathbf{x}')\nabla^2 p_{,\alpha}(\mathbf{x}')}} \ , \tag{26}$$

without summation over Greek indices. It is obviously impossible to derive a model of f which matches the DNS results for all the components. Hence, the following analysis should be interpreted in a qualitative rather than quantitative sense.

Figure 3 shows the correlation function $f(\mathbf{x},\mathbf{x}')$ corresponding to components ϕ_{11} (Fig. 3a) and ϕ_{22} (Fig. 3b) for 7 different y locations, at zero x- and z-separation. Each curve has been truncated for clarity, since the ratio (26) becomes rather "noisy" for large separations. Several observations can be made from the figure:

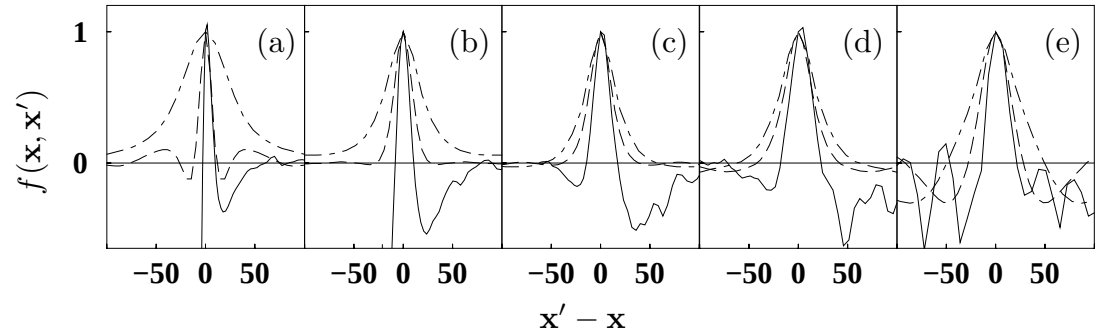

FIGURE 4. Comparison of shapes of the correlation function corresponding to ϕ_{22} for separations in the 3 principal directions at different locations. (a) $y^+ = 14$, (b) $y^+ = 30$, (c) $y^+ = 80$, (d) $y^+ = 150$, (e) $y^+ = 590$. Separations: —·— , x-direction, $(\Delta y = \Delta z = 0)$; ——— , y-direction, $(\Delta x = \Delta z = 0)$; - - - - , z-direction, $(\Delta x = \Delta y = 0)$.

- The correlation functions corresponding to ϕ_{11} and ϕ_{22} are quite different. In particular, the correlation length scale appears to be significantly larger at every location for the 11 component than for the 22 component.
- The correlation function becomes negative at certain separations, particularly for the 22 component.
- The correlation length scale varies with location. It increases rapidly when the fixed point $\mathbf{x}$ moves away from the wall. Then, it seems to reach a maximum level and decreases slightly as the center of the channel is approached. This behavior seems to be qualitatively the same for both components.
- These functions have asymmetrical shapes, particularly in the log layer. As pointed out in §4.1, the correlation function defined by (26) is not restricted to values less than or equal to 1. It can be observed in Fig. 3b that this is indeed the case. For instance, the correlation function at $y^+ = 400$ reaches a maximum value of approximately 1.15 at $y'^+ \simeq 405$.

The main conclusion which can be drawn from the figures is that the correlation function is very asymmetric. This feature is linked to the rapid variation of the length scale, which increases with distance from the wall. Modeling the correlation function by an exponential function leads to too much weight being placed in the region between the point and the wall. Therefore, as will be described below, the over-estimation of the pressure term in the log layer can be corrected by introducing some asymmetry in the model for $f(\mathbf{x}, \mathbf{x}')$.

5.3 Anisotropy of the correlation function

Figure 4 shows the correlation function corresponding to ϕ_{22}, evaluated from (26) with $\alpha = \beta = 2$, for separations in the principal directions. Note that for separations in y-direction the correlation function goes to $-\infty$ when the point y' approaches the wall, as can be seen in Figs. 4a and 4b. This is because in the ratio (26), the one-point correlation involves $u_2(y')$, which behaves as y'^2 in the vicinity of the wall, whereas the two-point correlation only contains $u_2(y)$ which is constant with respect to y'. Accordingly, the ratio behaves as y'^{-2} near the wall.

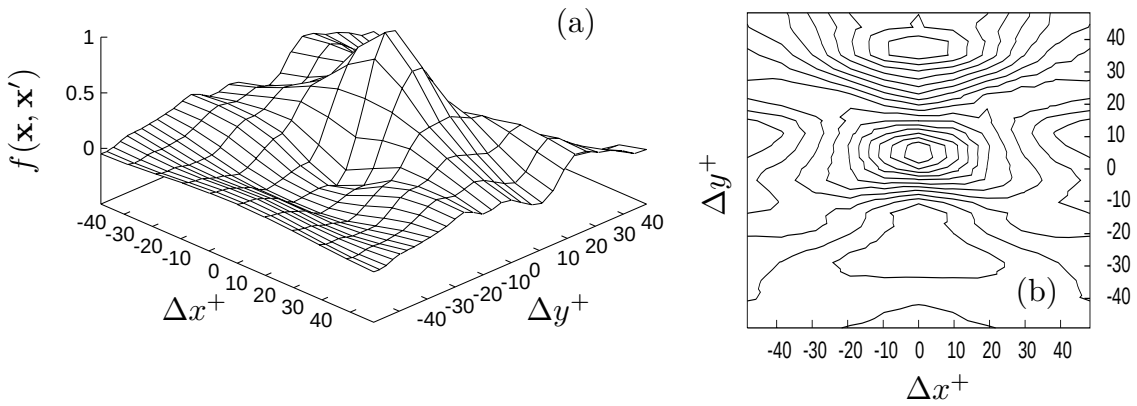

FIGURE 5. Correlation function corresponding to ϕ_{22} at $y^+ = 80$ for separations in the x-y plane ($\Delta z = 0$). (a) $f(\mathbf{x}, \mathbf{x}')$, (b) Iso-correlation contours. Contour levels from -0.5 to 1 are separated by 0.1.

All the Figs. 4a-e show that the velocity u_2 and the y-derivative of the Laplacian of the pressure are correlated over a longer distance in the streamwise direction than in other two principal directions. This feature is consistent with the streamwise elongation of the turbulent structures observed in the experiments. This anisotropy is very important near the wall (Fig. 4a) and becomes less pronounced away from it (Figs. 4b-e). Note that at the center of the channel, the correlation function is still anisotropic.

The anisotropy of the correlation function at location $y^+ = 80$, corresponding to Fig. 4c, can also be observed in Fig. 5. In 5a, $f(\mathbf{x}, \mathbf{x}')$ is plotted as a function of separation in the x-y plane ($\Delta z = 0$). Figure 5b shows the contour levels of this surface. One can observe that near the point of zero separation, the highest contour, which corresponds to $f(\mathbf{x}, \mathbf{x}') = 1$, is almost round. The shape of the contours becomes more elongated in the x-direction as the level decreases.

The asymmetry of the correlation function in y-direction, emphasized in §5.2, appears in Fig. 5b as well. When looking only at the spacing between consecutive contours, the function may seem somewhat symmetric. But it must be noted that the contours are not centered at the point of zero separation. Actually, the highest contour level plotted, $f(\mathbf{x}, \mathbf{x}') = 1$, contains this point. This asymmetry is clearly observed as well in the regions of negative contour values. First, they are not symmetrical with respect to zero, since they are approximately centered at $\Delta y^+ = -25$ and $\Delta y^+ = 35$. Secondly, the extremum of the region corresponding to positive separations is much lower than the other one.

The above observations demonstrate that the correlation function is not only asymmetric in the y-direction but also anisotropic, especially in the very near-wall region ($y^+ < 30$). Consequently, it calls into question the use of the exponential function, which does not distinguish between streamwise, wall-normal and spanwise directions. However, this anisotropy cannot be considered as being responsible for the defects noted in §4.1, since in the case of channel flow, the non-local effect obviously does not act in the homogeneous directions. Nevertheless, this points out

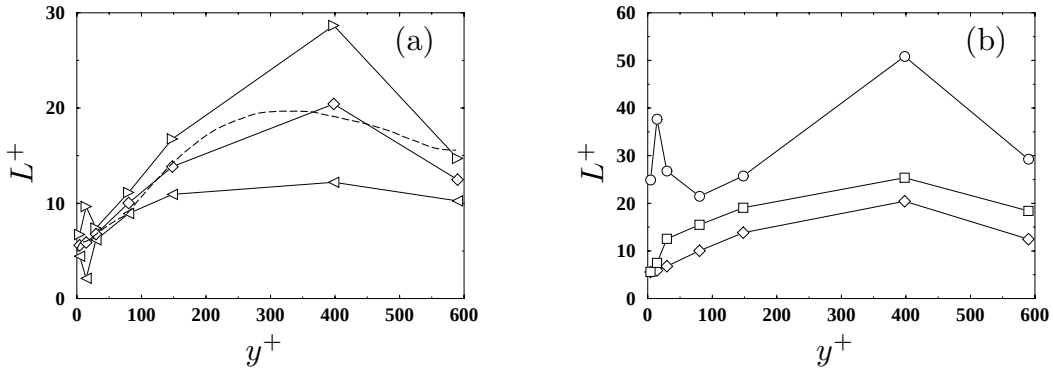

FIGURE 6. Length scales based on curves in Fig. 4. (a) Comparison of the different length scales in y-direction: ◁ Left length scale; ◇ Central length scale; ▷ Right length scale; ---- $L = C_L \max\left(k^{3/2}\varepsilon^{-1}, C_\eta \nu^{3/4}\varepsilon^{-1/4}\right)$ with $C_L = 0.045; C_\eta = 80.0$. (b) Comparison of the length scale in the 3 directions: ◇ Central length scale in y-direction; ○ Length scale in x-direction; □ Length scale in z-direction.

a feature of the correlation function which can become important in more complex flows.

5.4 The correlation length scale

The length scale L entering the model of the two-point correlations (13) is not easy to determine in DNS data. As emphasized in §4.1, it does not correspond rigorously to the integral scale (20).

It is noted that L is the integral of the function $\exp(-r/L)$ from zero to infinity. This property allows one to evaluate a length scale in each direction, but it is unfortunately not satisfactory. Since the x-direction is homogeneous, the integral over x of quantities involving x-derivatives is zero. Hence, the evaluation of the length scale in x-direction of the correlation function associated to ϕ_{11}, i.e., the function defined by (26) with $\alpha = \beta = 1$, gives exactly zero. This is due to the fact that it does not give the right weights to the different regions. Indeed, considering isotropic turbulence and ignoring the image terms, it can be seen that the 3-D integral (20) reduces to the 1-D integral $\int_0^\infty r f(\mathbf{x}, r) dr$, which increases the relative weight of the large separations.

The method which will be used in the following is not an integral method. It can be noted that the function $\exp(-r/L)$ takes the value $1/e$ for $r = L$. Thus, a length scale can be defined by the separation where the correlation function takes this value. Although this method is very simple, it provides a measure of the width of the function in each direction. The drawback is that it only characterizes the shape of the function at small separations and, in particular, it does not account for the negative excursions.

Nevertheless, this method allows the evaluation of the qualitative behavior of the length scale across the channel and distinguishes between the length scales evaluated at the left and right of the zero separation point, characterizing the asymmetry of the function. Figure 6 shows the different length scales which can be evaluated from the correlation functions depicted in Fig. 4. Figure 6a compares the different length

scales defined in the y-direction: the left (right) length scale corresponds to the value of negative (positive) separation at which the correlation function is equal to $1/e$, and the "central" length scale is the mean of the left and right length scales. It can be observed that, except for the peculiar behavior at $y^+ = 14$, the asymmetry is weak close to the wall and becomes more pronounced away from it. This trend is reversed when the center of the channel is approached.

The growth of the central length scale with y is nearly linear up to $y^+ = 200$. In Fig. 6a, the length scale used in the elliptic relaxation model is also plotted. It can be seen that the global shape is very satisfactory, although the coefficient C_L has been reduced by a factor of 4. This value of C_L cannot be considered as the value which must be used in the model, since it only corresponds to the component ϕ_{22}.

Figure 6b shows the evolution across the channel of the length scale in the 3 principal directions. Although their amplitudes are different, their behaviors appear quite similar, except for $y^+ < 100$, where a spike appears in the streamwise length scale.

These results indicate that the length scale used in the model, which is the standard turbulent length scale bounded by the Kolmogorov length scale, represents quite satisfactorily the variations of the correlation length in the channel. The coefficient C_L is likely over-estimated, but the results presented here are mainly qualitative and therefore, the coefficient tuned by computer optimization must be preferred. Overall, these results justify the way the length scale is modeled in the elliptic relaxation method. The use of the Kolmogorov length scale as a lower bound, which was originally introduced only to avoid singularities in the model, has proved important to improving the predictions of the model. This is due to the behavior of the correlation length described above, which does not go to zero and varies linearly in the vicinity of the wall.

6. Proposed modification to the model

6.1 Correction to the model of the correlation function

The results presented in the previous section show that the model of the correlation function can be improved. For the present study, whose main purpose is to find ways to correct the wrong behavior in the log layer as detailed in §4.1, the most noteworthy feature of the correlation function is its asymmetry in the y-direction. Indeed, Fig. 7 shows that, when the original correlation function model is used, the two-point correlation obtained by multiplying the model function by the one-point correlation from the DNS data (cf. (26)), is larger toward the wall than away from it. This is very different from the two-point correlation computed directly from the DNS fields, which is quite symmetrical. Consequently, the integral of the two-point correlation is over-estimated, leading to the incorrect amplification of the pressure term pointed out in §4.1.

This work does not attempt to find the best way to modify the model. Rather, it presents a direction in which an improvement of the model can be sought. An example of modification is presented in Fig. 7. The asymmetrical correlation function shown in 7b is obtained by introducing a dependence on the gradient of the

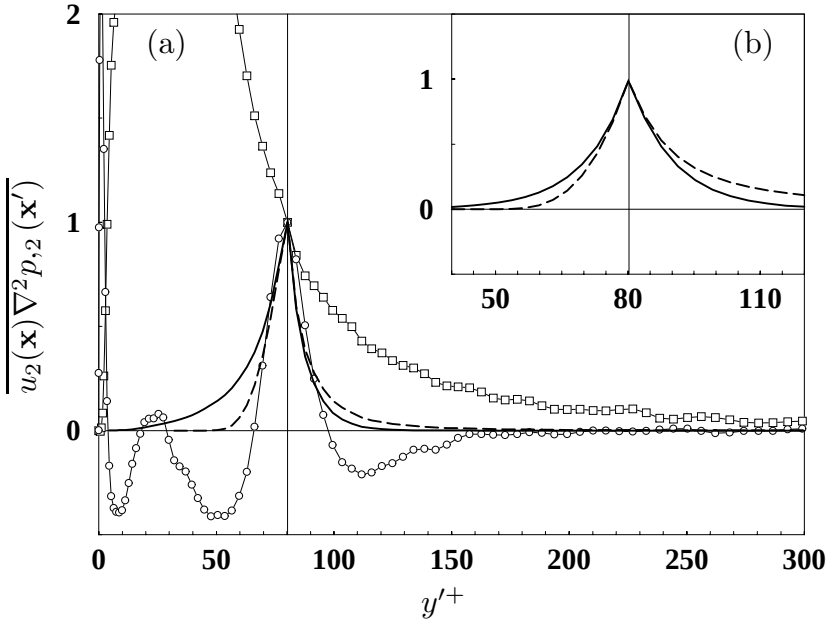

FIGURE 7. *A priori* test of the two-point correlation obtained using two different correlation functions. (a) One- and two-point correlations. All quantities are normalized by the value of the two-point correlation at zero separation. ▫ One-point correlation from DNS ($\mathbf{x} = \mathbf{x}'$); ∘ Two-point correlation from DNS; ——— Two-point correlation obtained using the symmetrical exponential correlation function shown in (b) and the one-point correlation from DNS; - - - - Two-point correlation obtained using the asymmetrical exponential correlation function shown in (b) and the one-point correlation from DNS. (b) Model of the correlation function. ——— Symmetrical correlation function: $f(y, y') = \exp(-|y' - y|/L)$; - - - - Asymmetrical correlation function: $f(y, y') = \exp(-|y' - y|/(L + (y' - y)dL/dy)$.

length scale: $f(y, y') = \exp(-|y' - y|/(L + (y' - y)dL/dy)$. The resulting two-point correlation, shown in 7a, is much closer to the DNS value than the one obtained using the original model. In particular, the new function corrects the erroneous shape observed between the point and the wall. The next section will detail the consequence of this new model on the form of the elliptic relaxation equation.

6.2 Reformulation of the elliptic relaxation equation

The simple modification of the correlation function model proposed above can easily lead to a new form of the elliptic relaxation model. The correlation function is henceforth modeled by

$$f(\mathbf{x}, \mathbf{x}') = \exp\left(-\frac{r}{L + r\mathbf{u}\cdot\nabla L}\right) \ , \tag{27}$$

where r and $\mathbf{u}$ denote respectively $\|\mathbf{x}' - \mathbf{x}\|$ and $(\mathbf{x}' - \mathbf{x})/\|\mathbf{x}' - \mathbf{x}\|$. Considering the new term $r\mathbf{u}\cdot\nabla L$ as a small correction, a Taylor expansion of (27) leads to the following expression:

$$f(\mathbf{x}, \mathbf{x}') = \exp\left(-\frac{r}{L}\right) + \frac{r^2}{L^2}\exp\left(-\frac{r}{L}\right)\mathbf{u}\cdot\nabla L \ . \tag{28}$$

Using (28), the integral equation of the pressure term leads to two terms ϕ_{ij}^a and ϕ_{ij}^b. The first term is the same as the original one and satisfies

$$\phi_{ij}^a - L^2\nabla^2\phi_{ij}^a = -\frac{L^2}{\rho}g_{ij} \ , \tag{29}$$

where g_{ij} denotes the one-point correlation $\overline{u_j\nabla^2 p_{,i}} + \overline{u_i\nabla^2 p_{,j}}$. The second term

$$\phi_{ij}^b = 8\frac{L^3}{\rho}\nabla L\cdot\nabla g_{ij} \tag{30}$$

is a correction term. Following Durbin (1991), the RHS of (29) can be replaced by any quasi-homogeneous model, which corresponds to modeling g_{ij} by $\rho\phi_{ij}^h/L^2$. There are two possible ways to take into account the correction term in the model. First, it can be considered as an explicit correction as

$$\phi_{ij}^a - L^2\nabla^2\phi_{ij}^a = \phi_{ij}^h \ ; \tag{31}$$

$$\phi_{ij}^b = 8L^3\nabla L\cdot\nabla\frac{\phi_{ij}^a}{L^2} \ . \tag{32}$$

Here, (31) gives exactly the same solution as the original model, while (32) provides an explicit correction. The second possibility is to introduce the correction directly into the elliptic relaxation equation in the following manner:

$$\phi_{ij} - L^2\nabla^2\phi_{ij} - 8L^3\nabla L\cdot\nabla\frac{\phi_{ij}}{L^2} = \phi_{ij}^h \ . \tag{33}$$

The same analysis as in §4.1 can be conducted in the log layer, which yields the following results:

(a) with the explicit formulation (31) and (32): $\phi_{ij} = \dfrac{1-24C^2\kappa^2}{1-2C^2\kappa^2}\phi_{ij}^h$;

(b) with the implicit formulation (33): $\phi_{ij} = \dfrac{1}{1+22C^2\kappa^2}\phi_{ij}^h$.

Both new formulations give a reduction of the redistribution, in contrast to the original one, which gave an amplification, as pointed out in §4.1. Note that the reductions are identical up to the third order in the small parameter $C\kappa$.

Thus, the simple modification of the model for the correlation function proposed above overcomes the deficiencies of the original model in the log layer. The so-called "wall echo effect", called into question in §5.1, can be obtained only by accounting for the asymmetry of the correlation function in the direction normal to the wall, i.e., by introducing a dependence on the gradient of the length scale in the model. This can be compared to the correction applied by Launder & Tselepidakis (1991), who sought to avoid the use of wall echo terms by introducing an "effective velocity gradient" in their pressure term model, defined as

$$\nabla U_i^{eff} = \nabla U_i + c^{eff}L(\nabla L\cdot\nabla)\nabla U_i \tag{34}$$

(see Wizman *et al.* (1996) for more details). This approach accounts for the inhomogeneity of the flow in the near-wall region, which is very similar to the present work.

7. Conclusions

A DNS database for a channel flow at $Re_\tau = 590$ has been used to assess the validity of the model assumptions in the elliptic relaxation method. Several conclusions can be drawn:

- The method, which is based on the approximation of the correlation function (26) by an exponential function, is consistent with DNS data, although some refinements are necessary. In particular, the length scale used in the model, defined by the standard turbulent length scale bounded by the Kolmogorov length scale, reproduces rather surprisingly the overall shape of that obtained from DNS data.
- The shape of the correlation function depends on the component of the two-point correlation tensor used to evaluate it. Therefore, one can not expect an accurate reproduction of all the two-point correlations. Only a global accounting of the non-local effect is possible.
- An analysis of the image terms entering the approximate Green function of the channel shows that they actually lead to an amplification, rather than reduction, of the redistribution between the components of the Reynolds stress, in contrast to the common belief. The reduction can only be due to the damping of the source term in the integral equation, especially for the diagonal component normal to the wall. Accordingly, this is not a wall echo effect, but a wall blocking effect.
- The correlation function computed from DNS data is strongly asymmetric in the direction normal to the wall, particularly in the log layer. Modeling it by a simple exponential function gives too much weight to the region between the point and the wall. Since the one-point correlation increases rapidly toward the wall, it yields an over-estimation of the pressure term. This is the reason for the observed erroneous amplification of the redistribution in the log layer.
- The correlation function is anisotropic. In particular, very close to the wall, the iso-correlation contours are strongly elongated in the streamwise direction. This feature has no influence on the channel flow, and its effect on complex flows cannot be determined in the present study.
- A simple modification to the correlation function model, accounting for the observed asymmetry in the direction normal to the wall, allows the derivation of a new formulation of the elliptic relaxation equation which does not possess the same defect as the original version. This result shows that the reduction of the redistribution in the log layer can be reproduced by introducing inhomogeneity effects and avoiding the use of any wall echo correction terms.

Based on the physical insight gained through this study, effort will continue to be directed toward the improvement of the elliptic relaxation method. Different formulations of the model will be tested in simple flows, in order to assess the improvement of the predictions. The new model will be calibrated on the channel flow and the boundary layer flow to allow its application in more complex configurations.

Acknowledgments

The authors gratefully acknowledge William Cabot, Javier Jimenez, and Robert

Moser for assistance with the DNS database and useful discussions.

REFERENCES

Bradshaw, P. 1973 The Strategy of Calculation Methods for Complex Turbulent Flows. *Imperial College, Dept. of Aero. Report.* **73-05,** 1-56.

Bradshaw, P., Mansour, N. N. & Piomelli, U. 1987 On Local Approximations of the Pressure-Strain Term in Turbulence Models. *Proc. Summer Program,* Center for Turbulence Research, NASA Ames/Stanford Univ., 159-164.

Chou, P. Y. 1945 On velocity correlations and the solutions of the equations of turbulent fluctuation. *Qrtly. of Appl. Math.* **3,** 38-54.

Durbin, P. A. 1991 Near-wall turbulence closure modeling without "damping functions". *Theoret. Comput. Fluid Dynamics.* **3,** 1-13.

Durbin, P. A. 1993 A Reynolds stress model for near-wall turbulence. *J. Fluid Mech.* **249,** 465-498.

Gibson, M. M. & Launder, B. E. 1978 Ground effects on pressure fluctuations in the atmospheric boundary layer. *J. Fluid Mech.* **86,** 3.

Kim, J. 1989 On the structure of pressure fluctuations in simulated turbulent channel flow. *J. Fluid Mech.* **205,** 421-451.

Kim, J., Moin, P. & Moser, R. 1987 Turbulence statistics in fully developed channel flow at low Reynolds number. *J. Fluid Mech.* **177,** 133-166.

Launder, B. E., Reece, G. J. & Rodi, W. 1975 Progress in the development of a Reynolds-stress turbulence closure. *J. Fluid Mech.* **68-3,** 537-566.

Launder, B. E. & Tselepidakis, D. P. 1991 Progress and paradoxes in modelling near-wall turbulence. *8th Symp. Turb. Shear Flows.* **29-1,** 1-6.

Lumley, J. L. 1975 Pressure-strain correlation. *Phys. Fluids.* **18**(6)**,** 750-750.

Mansour, N. N., Kim, J. & Moin, P. 1988 Reynolds-stress and dissipation-rate budgets in a turbulent channel flow. *J. Fluid Mech.* **194,** 15-44.

Monin, A. S. & Yaglom, A. M. 1975 *Statistical Fluid Mechanics.* MIT Press, English version of the original Russian version (1965).

Moser, R., Kim, J. & Mansour, N. N. 1998 Manuscript in preparation.

Parneix, S., Laurence, D. & Durbin, P. A. 1998 A procedure for using DNS databases. *J. Fluid Eng.* **120,** 40-47.

Sabot, J. 1976 *Etude de la cohérence spatiale et temporelle de la turbulence établie en conduite circulaire.* PhD thesis, Université de Lyon.

Wizman, V., Laurence, D., Kanniche, M., Durbin, P. & Demuren, A. 1996 Modeling near-wall effects in second-moment closures by elliptic relaxation. *Int. J. Heat and Fluid Flow.* **17,** 255-266.